Asociación Argentina
de Mecánica Computacional

Mecánica Computacional Vol XXIX, págs. 3225-3235 (artículo completo)
Eduardo Dvorkin, Marcela Goldschmit, Mario Storti (Eds.)
Buenos Aires, Argentina, 15-18 Noviembre 2010

THE TECHNIQUE OF ACTIVE/INACTIVE FINITE ELEMENTS FOR THE ANALYSIS AND OPTIMIZATION OF ACOUSTICAL CHAMBERS

Renato Barbieri[a], **Nilson Barbieri**[a,b], **Key Fonseca de Lima**[a]

[a]*Pontificia Universidade Católica do Paraná-PUCPR- Programa de Pós-Graduação em Engenharia Mecânica - Rua Imaculada Conceição, 1155 – Prado Velho – Curitiba – Paraná – Brasil - http://www.pucpr.br/cursos/programas/ppgem*

[b]*Universidade Tecnológica Federal do Paraná – UTFPR – Departamento de Engenharia Mecânica- Rua Sete de Setembro, 3165 – Rebouças - Curitiba – Paraná - Brasil, http://www.damec.ct.utfpr.edu.br/*

Keywords: Active finite element, genetic algorithm, optimization, acoustical chamber.

Abstract. In this work are investigated two topics associated with numerical calculations of the acoustic transmission loss in acoustical silencers: analysis of acoustic chambers employing active/inactive finite elements and its optimization using the GA with integer variables. The technical information on the use of active/inactive elements and the definition of all the design variables used for the entire control of the finite element mesh are detailed. Although simple, the numerical results for the examples analyzed show excellent convergence achieved with the combination of these two techniques for the optimization of symmetrical acoustic chambers.

1 INTRODUCTION

The transmission loss, TL(ω), can be used to define the problem of optimization of acoustic chambers (mufflers) as (Luenberger, 1989; Bazaraa et. all., 1993):

$$\begin{array}{lll} \text{Maximize or Minimize} & f(TL(\omega)) & \\ \text{Subject to} & x_{jL} \le x_j \le x_{jU} \qquad j=1,2,3,...,nd & (1) \end{array}$$

where f(TL(ω)) is the objective function that depends of the excitation frequency ω and the nd variables of design x_j with lower limit x_{jL} and upper limit x_{jU}.

To perform the optimization of the acoustic chamber on discrete frequencies is defined an objective function with discrete values of the transmission loss as:

$$f(\omega_1, \omega_2, ..., \omega_n) = \sum_{i=1}^{n} \alpha_i TL(\omega_i) \tag{2}$$

where α_i represents a positive penalty parameter defined with the purpose of enhancing the value of transmission loss in a specific frequency ω_i.

For the optimization in all frequency range the objective function can be written using the average transmission loss in different frequency ranges. Mathematically this function is expressed in the following way (Barbieri and Barbieri, 2006):

$$f(\Delta\omega_1, \Delta\omega_2, ..., \Delta\omega_n) = \sum_{i=1}^{n} \alpha_i \overline{TL}(\Delta\omega_i) \tag{3}$$

where

$$\overline{TL}(\Delta\omega_i) = \frac{1}{\Delta\omega_i} \int_{\omega_{iL}}^{\omega_{iU}} TL(\omega)\, d\omega \tag{4}$$

and α_i represents a positive penalty parameter defined with the purpose of enhancing the value of transmission loss in a specific frequency range $\omega_{iL} \le \Delta\omega_i \le \omega_{iU}$.

After selecting an appropriate objective function and the definition of design variables and their limits, the mathematical problem defined in Eq (1) can be solved using traditional optimization methods in the literature.

In this work was used the finite element method to evaluate the objective function together with the concept of active/inactive finite element to make the control of the mesh. The method of GA with integer variables was used to perform the optimization calculations and the great advantage of this approach is the reduced processing time. All methodology with use of active/inactive elements and the definition of design integer variables used in the GA are detailed later in this paper. Although simple, the numerical examples shown in this paper are to point out the quality of the results obtained with this approach.

2 THE CONTROL OF THE MESH AND THE DEFINITION OF DESIGN VARIABLES

After the construction of a homogeneous mesh of finite elements is defined a region where it want to control the geometry in order to optimize the design. Figure 1 show a shaded region

composed to nd columns with 10 finite elements per column. This is the *design domain*.

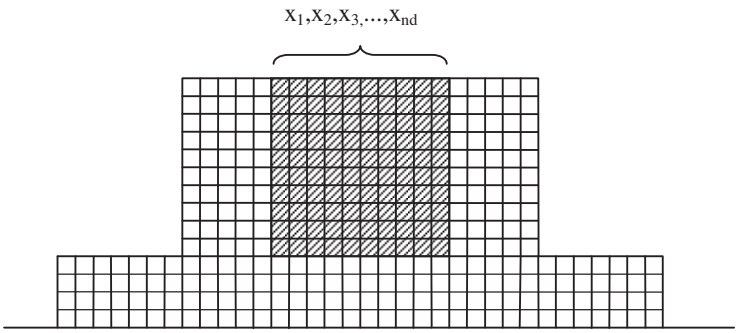

Figure 1 – Mesh of finite elements and the *design domain*.

Analogous to the process of topology optimization widely used in structural optimization, the finite element within the design domain are called to active or inactive elements. The active elements are those where the Helmholtz equation is usually modeled with FEM and inactive elements are those where the characteristic matrices of finite element are null.

Each column in the design domain has Nj elements that corresponds to the upper limit of the design variable xj, j = 1,2 ,..., nd. In Figure 1, Nj = 10 for any column.

The design variables are used to define the number of inactive elements in each column of the design domain. Thus each xj is an integer variable and $1 \leq xj \leq Nj$. Figure 2 shows that xm = 8 indicating that there are only 8 inactive elements (filled with black color) in the column m = 5 of the design domain.

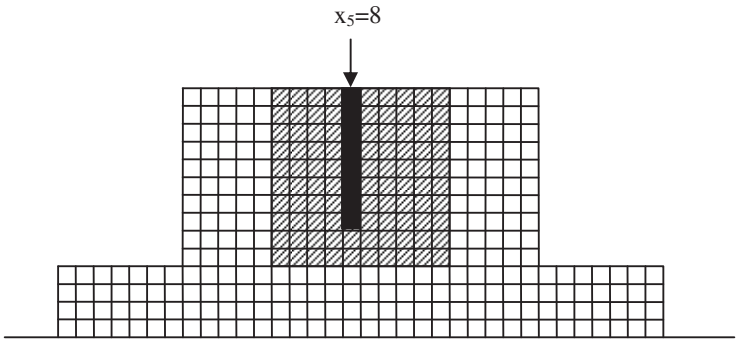

Figure 2 – Inactive elements in the column m (filled with black color).

After assembling all the elements, some rows and columns of the finite element matrix can have all null elements. These rows and columns are associated to the nodes inside the design domain that belong only to inactive elements. Therefore, to avoid the singularity of the final system of equations is sufficient to specify to these diagonals any nonzero value. This procedure does not change the result of the analysis, because these nodes are completely uncoupled (inactive node) of the other nodes of the mesh and pertain to inactive elements that are not post-processed. In Figures 3a and 3b are illustrated examples of this situation to meshes build with linear and quadratic elements, respectively. These figures show the shaded inactive elements and inactive nodes filled with black color. However, the approach described above can be applied to any other type of element.

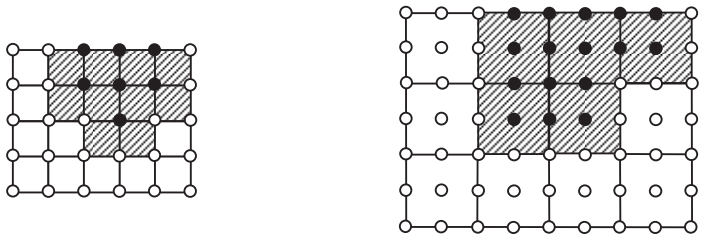

(a) (b)

Figure 3 – Uncoupled nodes during the optimization process. (a) Mesh with linear finite elements and (b) mesh with quadratic finite elements.

During all the optimization process the finite element mesh remains unchanged, but for each evaluation of the objective function some active elements may become inactive and vice versa, because there are changes in the values of design variables. As the mesh does not change the final value of the objective function depends of Δh that defines the size of the elements of each of the columns pertain the design domain. The point of optimum obtained with these integer variables tends to the value obtained with real variables when Δh tends to zero (very refined mesh). It is clear that the use of very refined mesh increases substantially the processing time of the analysis, due to the fact that increasing the number of degrees of freedom model and the integral used to evaluate the objective function is solved numerically. Therefore, an h-adaptive refinement is indicated to obtain small values for Δh that defines the size of the element mesh and the desired accuracy of the calculations.

3 NUMERICAL EXAMPLES

All the examples illustrated in this work were calculated using the following characteristics for the GA: crossover probability of 50%; probability of permutation of 2%, in each generation were evaluated 25 times the objective function and maintaining the characteristics of elitist reproduction.

The computational finite element and GA routines were developed by the authors and written in Fortran 90. The Lagrangean element of 9 nodes was used in all tests and the properties of the medium were c=346 m/s and ρ=1,21 kgf/m^3.

3.1 Example 1

In this example it is shown the optimization of a single chamber with extended inlet/outlet ducts. The single chamber has the following geometric data: D=150 mm for the chamber diameter, $d_1=d_2$=50 mm for the inlet/outlet ducts, and L=300 mm for the chamber length.

With these geometric features and considering c = 346 m/s, the first two frequencies of this chamber where the null acoustic attenuation are f_1=c/2L=576,66 Hz and f_2=c/L=1153,33 Hz. Based on this information it selects two frequency ranges to maximize the TL(ω) with the following objective function:

$$f(\Delta\omega_1, \Delta\omega_2, ..., \Delta\omega_n) = \sum_{i=1}^{n} \alpha_i \overline{TL}(\Delta\omega_i) = \frac{1}{50} \int_{550}^{600} TL(\omega)d\omega + \frac{1}{100} \int_{1100}^{1200} TL(\omega)d\omega$$

where the integrals are numerically calculated with the known Simpson rule and TL(ω) is evaluated with step of 5 Hz. In this way, are necessary 11 calculations of TL(ω) to evaluate the first integral and 21 calculations to evaluate the second integral.

In the evaluation of TL(ω) is used the finite element mesh quadratic (9 nodes) illustrated in Figure 4. Are defined only two design variables (x1 and x2) to control the h1 and h2 lengths of the inlet/outlet extended ducts. These design variables defines the number of inactive elements of the finite element mesh that appear filled with black color in this figure. Therefore, the limits for these design variables (integers) defined for the solution of this example are $1 \le x_1 \le 30$ and $1 \le x_2 \le 25$, because the mesh is homogeneous with element size of Δh=5mm. Although this is a mesh with small number of elements the results can be considered reliable until the frequency of 3000 Hz which is the upper value shown in Fig. 5. The analysis of phase errors (numerical x analytical) and amplitude to the problems of linear acoustics is widely studied in the literature, for example: Ihlemburg et al. (1997) e Barbieri et. al. (2004). Barbieri et al. (2004) found maximum amplitude error of 0.01% and 0.1% for the phase between the analytical and numerical solution in the quasi-singularity. Near the singular point is expected minor error: 0.004% for amplitude and 0.01% for the phase. These values were obtained using 23 elements per wavelength (3000 Hz) and due to error curves shown in this reference.

The design variables x_1 and x_2 are calculated as the integer part of $h_1/\Delta h$ and $h_2/\Delta h$. Therefore, the maximum number of evaluation of the objective function to find the optimal solution to this finite element mesh is at most equal to 30×25=750. In relation to the optimal values calculated with real variables it is expected maximum error in h1 and h2 of 2.5 mm which corresponds to half the characteristic size of the element.

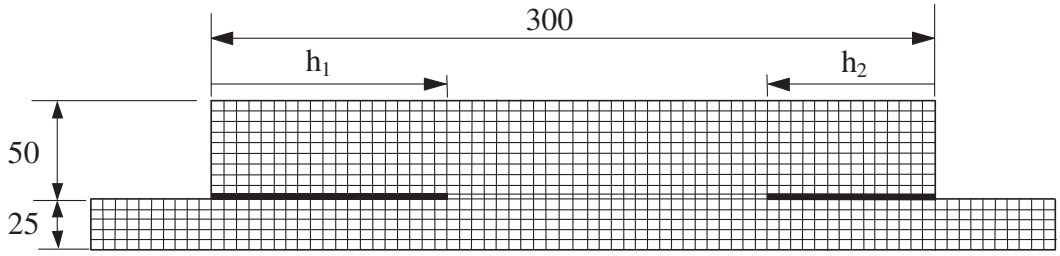

Figure 4 – Finite element mesh and design variables (real).

The convergence is achieved in the first generation (iteration) with 25 evaluations of the objective function. Figure 3 shows the two regions used to define the optimization intervals (550-600 Hz and 1100-1200 Hz) and the TL(ω) curves for the single chamber (h_1=h_2=0) and to the optimized chamber using extended inlet/outlet ducts (h_1= 40 mm and h_2= 60 mm). It can be noted that between 1100 and 1200 Hz there is a low attenuation of optimized TL(ω) curve due to use of elements with size of 5 mm. Results for this optimization problem using real variables can be found in Barbieri and Barbieri (2006) and show that these low attenuations in TL(ω) can be eliminated by refining the mesh.

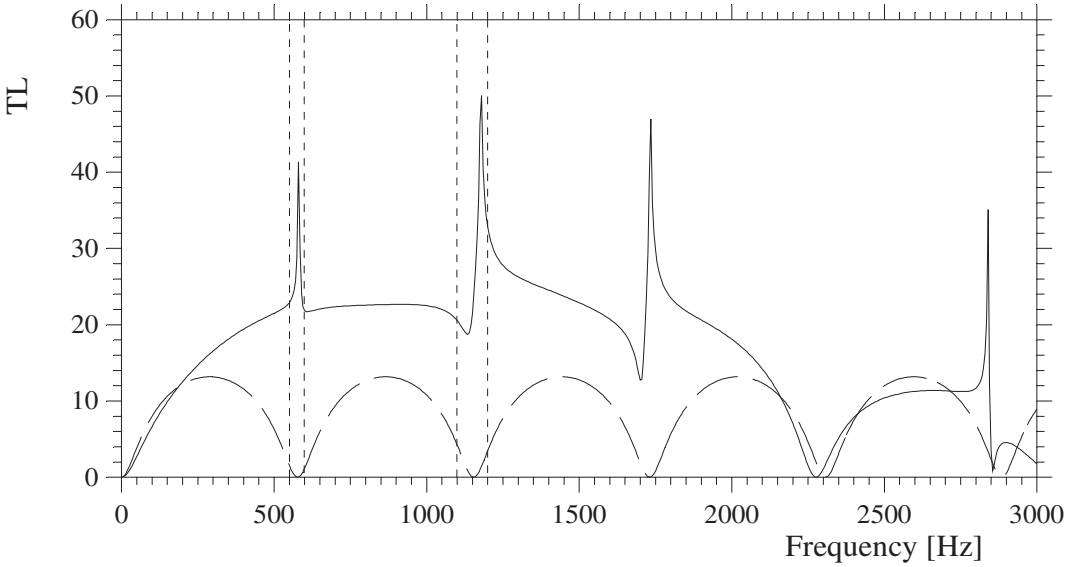

Figure 5 – TL(ω) for single chamber (dashed line) and for optimized chamber with extended inlet/outlet ducts (solid line).

3.2 Example 2

In the results shown in Fig. 5 is easily noted that the acoustic attenuation in the frequency range from 2200 to 2400 Hz is lower and a new optimization was performed in order to eliminate this disadvantage. The strategy employed was to use mini-chambers in the inlet duct in order to not significantly alter the volume of the chamber and does not cause substantial changes in the TL(ω) curve. Similar strategy was used by Lima (2008) who used corrugated pipes to eliminate this kind of problem with satisfactory results.

In Figure 6a is show the design domain used to new optimization problem and Figure 6b shows the design variables and the illustration of a homogeneous mesh with $\Delta x=\Delta y=5$mm where the filled elements represent the inactive elements.

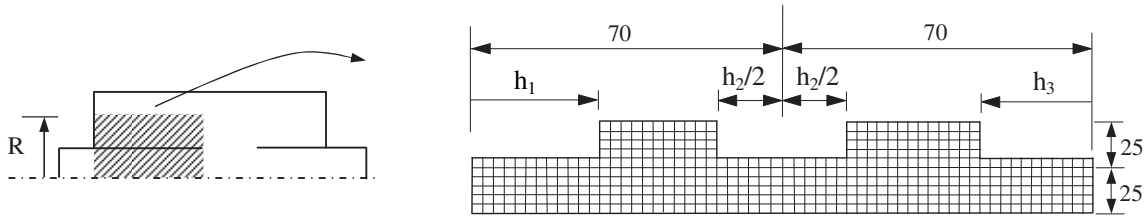

a) Design domain. b) Design variables and control of mesh.

Figure 6 – Geometry, finite element mesh and design variables.

The optimization process was carried out using homogeneous mesh with $\Delta x=\Delta y=2,5$mm and the geometric constraints imposed to the design variables (integers) were defined as $2\leq x_1\leq 16$; $2\leq x_2\leq 16$ and $2\leq x_3\leq 16$. The frequency range used to calculate the objective function was 2150 to 2450 Hz and the final geometry found is illustrated in Fig. 7 where the elements filled with black color indicate the inactive elements (walls). The convergence to the optimum values was also achieved at the end of the first generation (25 iterations).

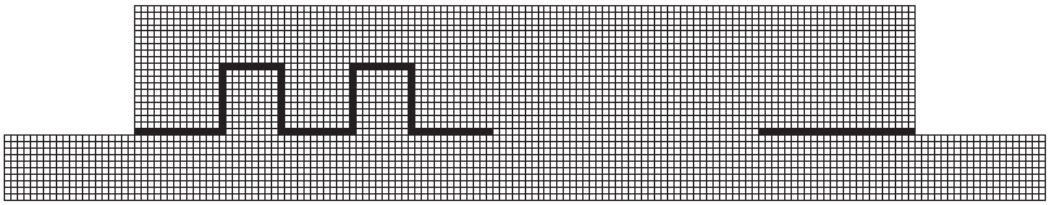

Figure 7 – Geometry and finite element mesh after optimization.

The values found for the design variables were h_1= 32.5 mm ; h_2= 25 mm and h_3= 30 mm with f=44,806 dB. The TL(ω) curve obtained with this new geometry is show in Fig. 8 and it can be noted significant increase of TL(ω) in the frequency range of 2000 to 3000 Hz and lower changes in other regions were already expected in function of change in the in internal volume of the chamber.

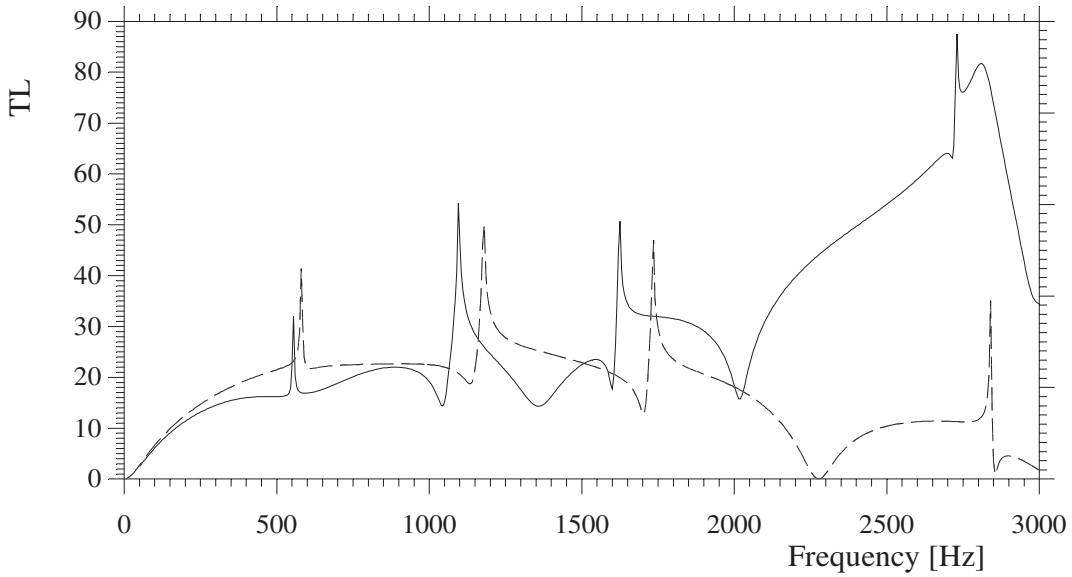

Figure 8 – TL(ω) for optimized chamber with inlet/outlet extended ducts (dashed line) and with mini-chambers in the input (solid line).

3.3 Example 3

In this example is show the optimization of the same simple camera used in Example 1, but the frequency range used in the optimization was 350 Hz to 400 Hz and was defined 60 design variables to define the region area. Each of these design variables takes the value 0 (inactive) or 1 (active). The inactive elements indicate the existence of material (wall) and the active elements indicate free passage of airflow. In Figure 9 is illustrated the situation where all elements of the design domain are inactive.

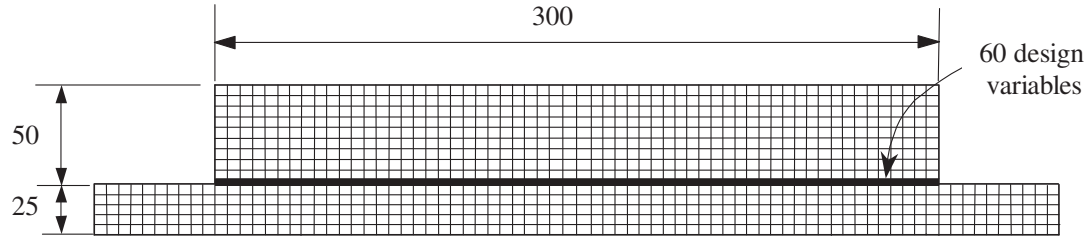

Figure 9 - Finite element mesh and design variables (real).

The optimization was performed using 20 evaluations of the objective function for each generation and the objective function was calculated using $\Delta\omega$=5Hz and the same finite element mesh of example 1. The optimum geometry obtained using these conditions is shown in Figure 10 and it was reached after 8 generations (160 evaluations of the objective function) as shown in Fig.11. The TL(ω) curve for these conditions is shown in Fig.12 which is also shown the frequency range used in the optimization process.

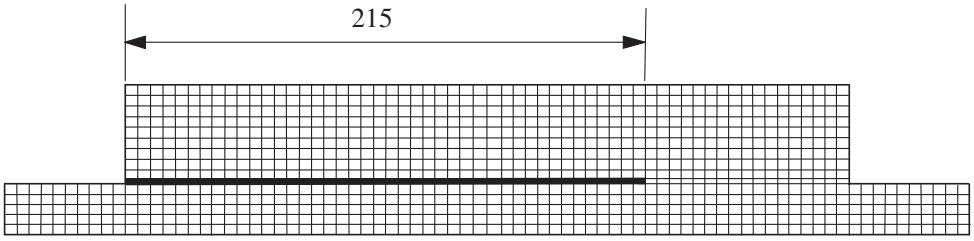

Figure 10 - Geometry and finite element mesh after optimization.

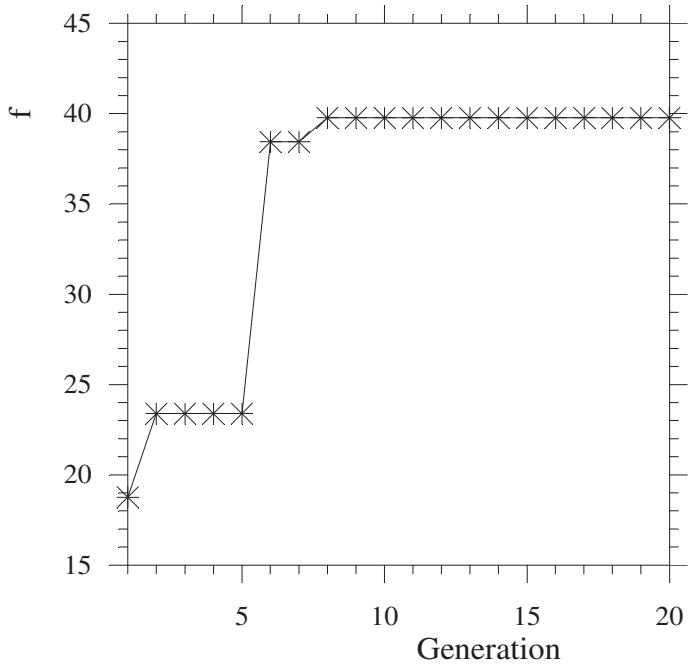

Figure 11 – Convergence analysis for example 3.

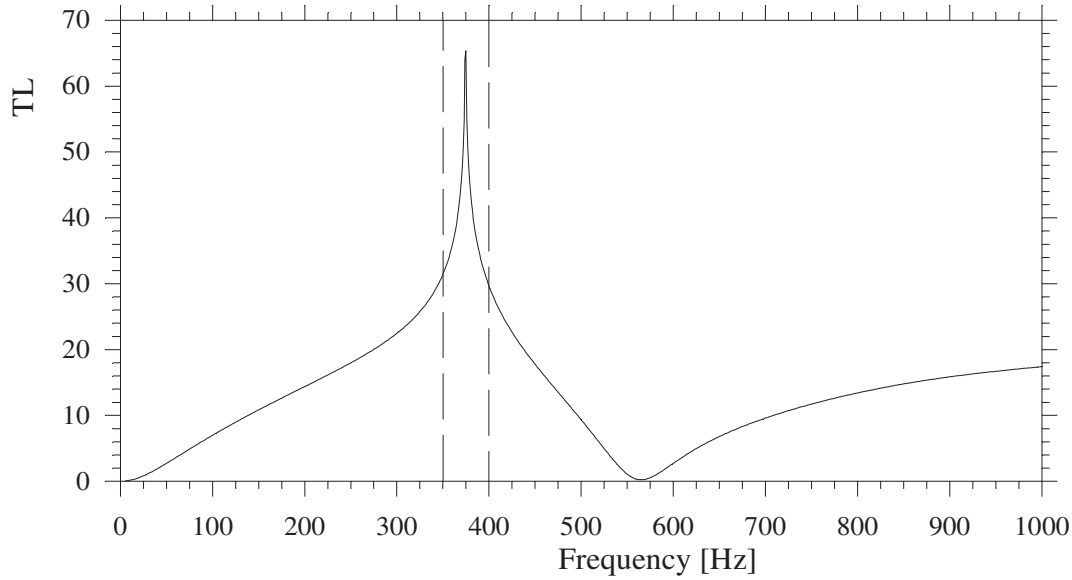

Figure 12 – TL(ω) curve after optimization and frequency range used in the optimization process.

3.4 Example 4

In this application are used 3 design variables for the optimization of the double extension chamber with extended pipes in the internal division, Figure 13. The dimensions of the

chamber and inlet/outlet ducts are the same as the previous example. The finite element mesh also has a characteristic size of 5 mm and the limitation of the 3 real design variables are given by $h_1 \leq 160$; $h_2 \leq h_1 - 5$ and $h_3 \leq 295 - h_1$ and they are associated with 3 integer design variables: $1 \leq x_1 \leq 32$; $1 \leq x_2 \leq x_1 - 1$ and $1 \leq x_3 \leq 59 - x_1$.

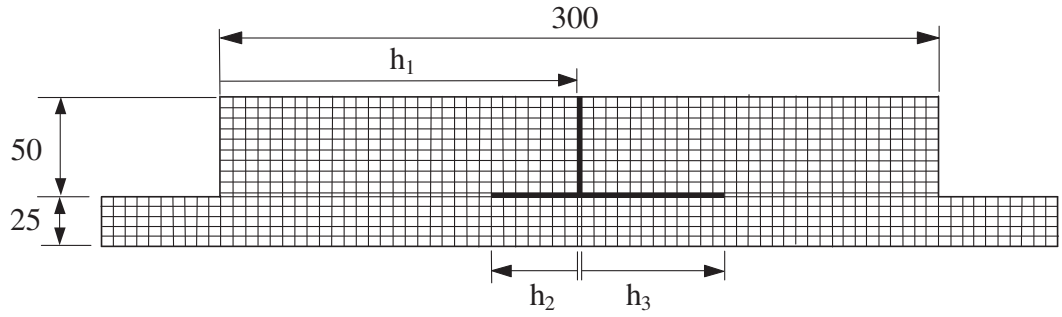

Figure 13 – Finite element mesh and design variables.

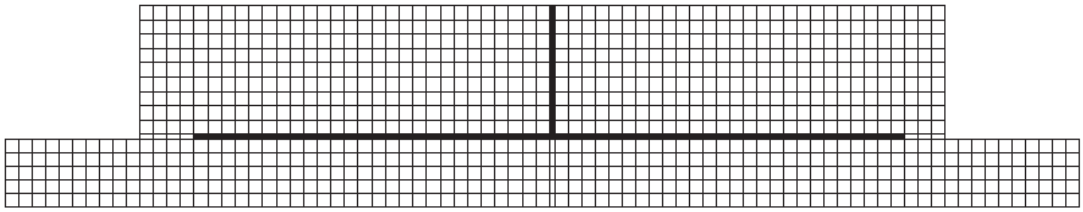

Figure 14 - Geometry and finite element mesh after optimization

The optimum values were also found at the end of the first generation and they were equal to f = 47.36 dB, h1 = 150, h2, and h3 = 130 = 127.5. The difference between h2 and h3 is the value of the central wall thickness (2.5 mm) and as the mesh has elements with 5 mm of length there is no possibility of greater accuracy than this. The geometry and finite element mesh for the optimum values that shown in Fig.14 and the TL(ω) curve for this situation is shown in Fig.15. Again, probably better results could be obtained by refining the mesh.

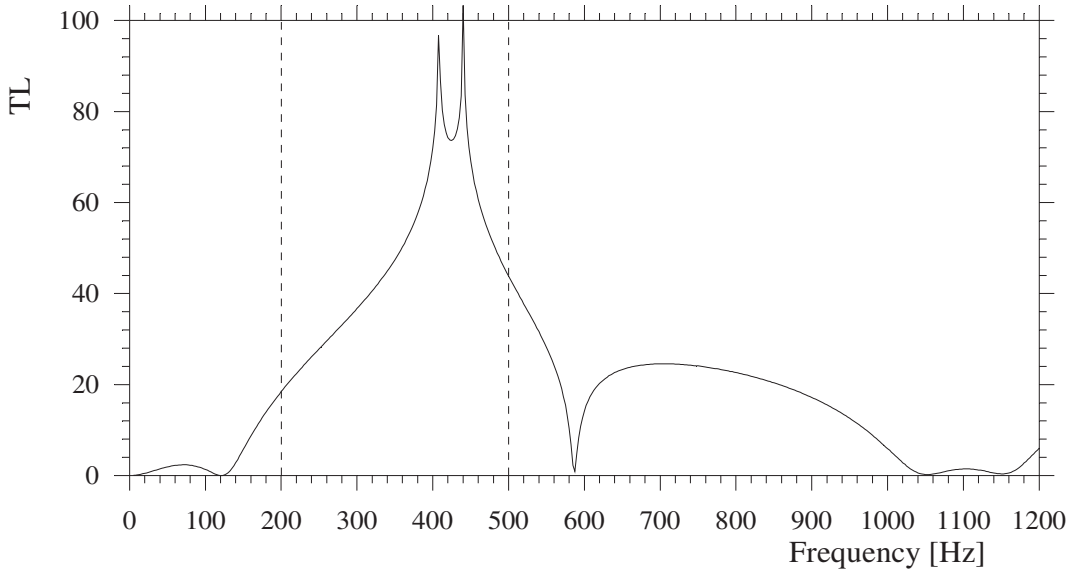

Figure 15 – TL(ω) after optimization.

4 CONCLUSIONS

The conclusions from the results shown above are:

1. The quality of results obtained with the technique of active/inactive finite elements is associated with the size of the element. Best results are obtained for smaller meshes;

2. The control of mesh for each stage of optimization is quite simple and extremely fast;

3. The GA with integer variables produces satisfactory results and good convergence. Examples 1.2 and 4 converged to the optimal geometry in the first-generation;

4. Even using 60 design variables the convergence shown in Example 3 was also very good.

REFERENCES

Barbieri, R. and Barbieri, N. Finite element acoustic simulation based shape optimization of a muffler. *Applied Acoustics*, 67:346–357, 2006.

Barbieri, R; Barbieri, N. and Lima, K.F. Application of the Galerkin-FEM and the improved four-pole parameters method to predict acoustic performance of expansion chambers. *J. of Sound and Vibration*, 276:1101–1107, 2004.

Bazaraa, M. S.; Sherali, H. D. and Shetti, C. M., *Nonlinear programming*. New York: Wiley; 1993.

Ihlenburg, F.; Babuska, I. and Sauter, S. Reliability of finite element methods for the numerical computation of waves. *Adv Eng Soft*, 28:417-424, 1997.

Lima, K. F., *Metodologia de Avaliação de Filtros Acústicos Reativos.* Tese de doutorado. Universidade Federal de Santa Catarina. 2008

Luenberger, D. G., *Linear and nonlinear programming*. Reading (MA): Addison-Wesley, 1989.